ELSEVIER

Polymer 43 (2002) 3083–3091

polymer

www.elsevier.com/locate/polymer

Fracture behaviour of polypropylene films at different temperatures: fractography and deformation mechanisms studied by SEM

Didac Ferrer-Balas[a], Maria Lluïsa Maspoch[a,*], Yiu-Wing Mai[b,c]

[a]*Departament Ciència dels Materials i Enginyeria Metal lúrgica, Centre Català del Plàstic, Universitat Politècnica de Catalunya, Av. Diagonal 647, 08028 Barcelona, Spain*

[b]*School of Aerospace, Mechanical and Mechatronic Engineering, Centre for Advanced Materials Technology (CAMT), University of Sydney, Sydney, NSW 2006, Australia*

[c]*MEEM, City University of Hong Kong, 83 Tat Chee Avenue, Kowloon, Hong Kong*

Received 1 August 2001; received in revised form 2 January 2002; accepted 14 January 2002

Abstract

The fracture surfaces and the deformation micro-mechanisms of one polypropylene homopolymer and three ethylene–propylene block copolymers (EPBC) have been studied by scanning electron microscopy. The results are compared to the essential work of fracture parameters obtained in a previous study with deeply double-edge-notched-tension samples of films fractured between −40 and 70 °C. The homopolymer shows shear-yielding at $T \geq -20$ °C, but at lower T, crazing prevails. The EPBC display shear-yielding for $T > 0$ °C, while a combination of cavitation and shear-yielding occurs at lower T, which is responsible for stress-whitening. The variations of the specific essential fracture work and specific plastic work with T and with ethylene content have been successfully explained in terms of the prevalent deformation mechanisms.

Keywords: Polypropylene; Essential fracture work; Ethylene–propylene block copolymers

1. Introduction

The essential work of fracture (EWF) method has been successfully applied to ductile and tough polymers in the last 15 years by many research groups [1–9] and is based on the separation of the energy contributions into two specific terms, the specific essential work (w_e) and the specific plastic work (βw_p) (the theoretical development of energy partitions can be found elsewhere [9]). According to the theory [10], w_e for the inner fracture process zone (FPZ) is a material parameter (surface-related) which depends on the sheet thickness but not on geometric factors and it is a material toughness for that thickness. But βw_p (volume-related) is not an intrinsic property (and it depends on specimen geometry). Usually, deeply double-edge-notched-tension (DENT) specimens are used for testing. Physically, w_e involves the specific work required for the creation of two new surfaces, and deformation processes occurring at the fracture plane as ligament yielding and localised necking, all of which occur in the FPZ. βw_p is related to the irreversible work dissipated in a surrounding or outer plastic zone (OPZ). β is a shape factor for the OPZ. The determination of β, and thus of w_p, is not always obvious, however.

In a previous paper [9], the fracture of films of one polypropylene (PP) homopolymer and three ethylene–propylene block copolymers (EPBC) with different ethylene content (EC) at temperatures around the PP glass transition ($T_g \sim 0$ °C) was investigated by means of the EWF method. The fracture behaviour was studied at a low speed (2 mm/min) in the temperature range from −40 to +70 °C. The EWF fracture parameters (w_e and βw_p) of the homopolymer were found to be much more temperature-sensitive than the EPBC with lower EWF values at $T < T_g$ and the opposite trend at $T > T_g$. The ductile–brittle transition of the homopolymer, that occurs below its T_g, was suppressed for the EPBC in the temperature range studied. The variations of the EWF parameters with T were explained in terms of molecular relaxations, ethylene phase content, and changes in the yield and fracture stresses.

In this paper, different observations by scanning electron microscopy (SEM) were carried out to aid in a better understanding of the EWF results found in our previous study [9] and the relationships between these parameters and deformation micro-mechanisms.

* Corresponding author. Tel./fax: +34-934-016-706.
E-mail address: maspoch@cmem.upc.es (M.L. Maspoch).

0032-3861/02/$ - see front matter
PII: S0032-3861(02)00102-7

2. Materials

The PP commercial grades chosen were one homopolymer (called H0) and three low EC block copolymers (EPBC), with 5.5, 7.4 and 12 wt% of ethylene (called C1, C2 and C3, respectively), as determined by Fourier transformed infrared spectroscopy. The material was received as pellets, and cast-extruded to obtain 90 μm nominal thickness (t) non-oriented films. To homogenise the crystal microstructure of the material, which is basically smectic (or quenched) after rapid cooling [11], the films were annealed for 1 h in a fan-assisted oven at 120 °C (controlled to ±2 °C), producing a transformation of the smectic phase to a monoclinic state. The preparation procedure and testing of the DENT specimens were described elsewhere [9].

3. Experimental work

The fractured ligament was observed in two different planes using SEM on post-mortem specimens after being gold-coated. Fig. 1(a) shows the fracture surface seen from the top in which two regions were observed, that near the notch edge (called *notch*) corresponding to the initial stage of the propagation, and that in the central area (called *central*) related to the terminal propagation stage. Fig. 1(b) shows another plane normal to the fracture ligament for the analysis of sub-surface deformation mechanisms.

4. Results and discussion

4.1. Fractography

Fractographic study helps to understand the fracture processes occurring in a DENT specimen. When the notched specimen was tested (at a low strain rate), the ligament yielded before crack growth (visible by stress-whitening seen in the copolymers). This loss in transparency is related to deformation processes occurring in the material, which require energy dissipation due to localised reduction in thickness in the ligament area and, subsequently, to crack growth initiation. During crack growth, the already yielded material contained in the ligament continues to deform, particularly at the crack-tip, until fracture. Thus, the fractographic analysis, Fig. 1(a), gives information about the fracture surface work and the work of necking (measured by the final sheet thickness). As an example, the notch area can be compared between H0 tested at −40 °C (Fig. 2(a)) and C2 tested at 50 °C (Fig. 2(b)), where the effect of both T and EC can be observed as a dramatic increase in ductility and plastic deformation. Note that, in each of Figs. 2–10, an inset has been included with a micrograph of the ligament area of post-mortem DENT specimens, with an arrow indicating the exact zone from which the SEM picture is taken. The presence of *shear lips*, observable in all fractured specimens, indicates the predominantly plane-stress condition prevailing in the films during the tests. It is particularly interesting to see that in the least plane-stress case (the most rigid material, H0, tested at −40 °C), these shear lips appear clearly (Fig. 2(a)). It is noted that the plane-stress state is responsible for a shifting of the ductile–brittle

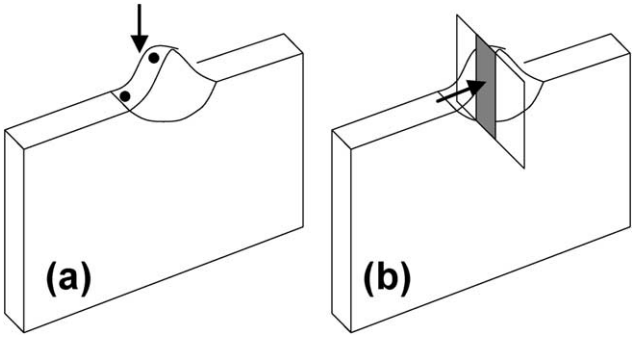

Fig. 1. Schematic of SEM surfaces observed on post-mortem DENT specimens. The arrows indicate the observation direction. (a) Direct observation of fracture surfaces. The dark points indicate the different regions of observation (called notch and central). (b) Schematic of the section that was obtained to observe the deformation micro-mechanisms in the specimen core region.

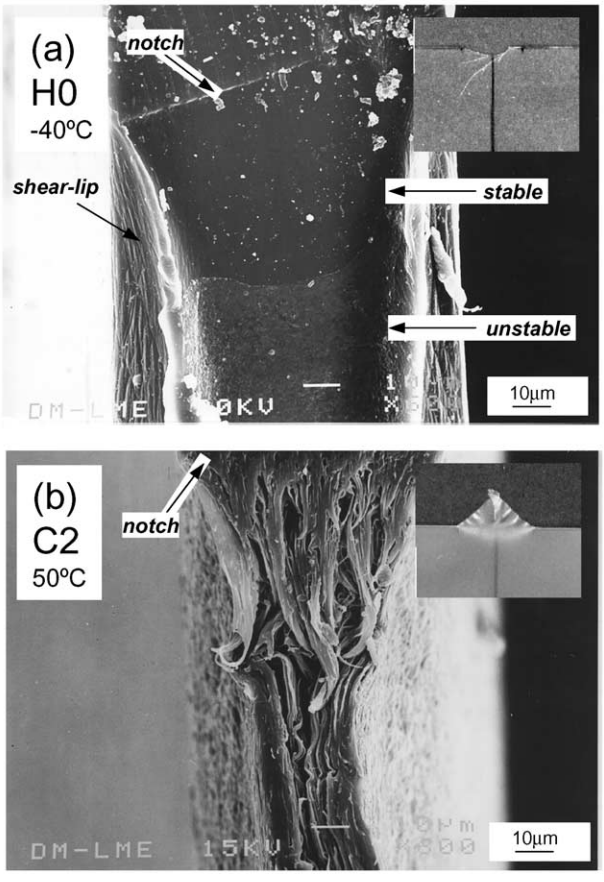

Fig. 2. Examples of fracture surfaces observed by SEM in two different specimens. (a) H0 tested at −40 °C, showing unstable behaviour and different fracture surface regions. (b) C3 tested at 50 °C, showing stable fracture with high ductility.

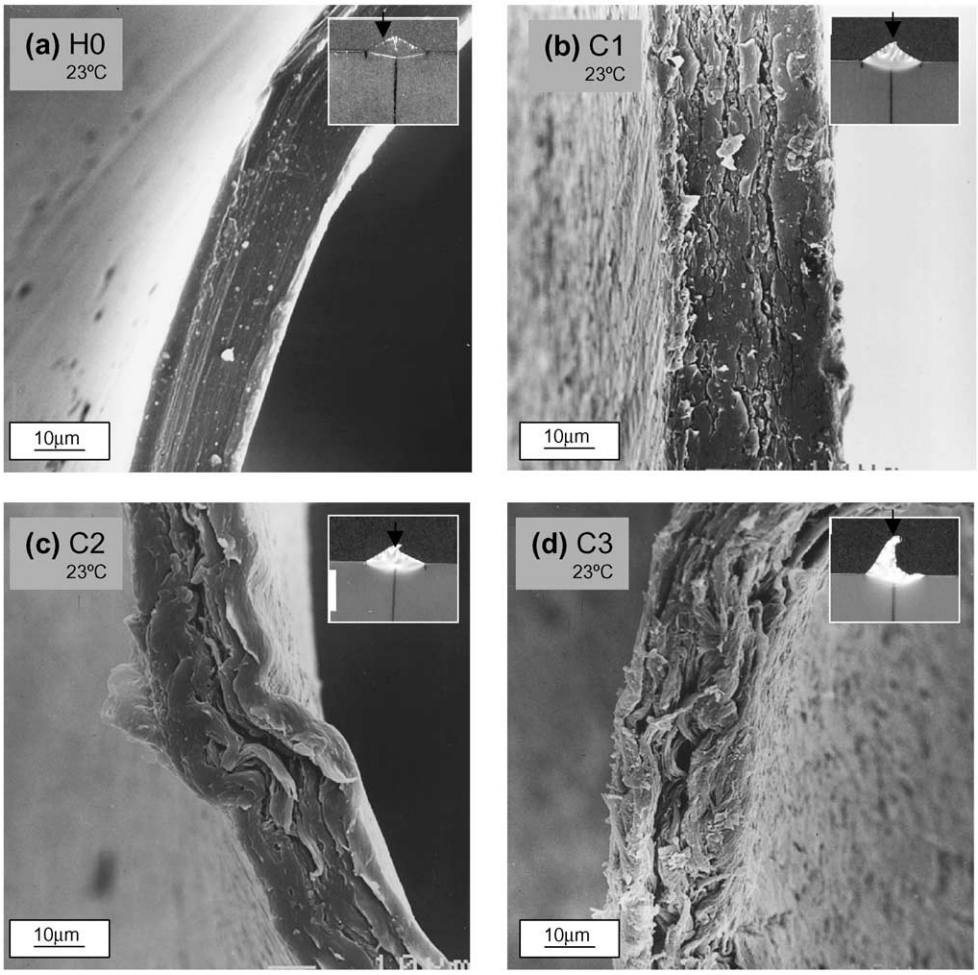

Fig. 3. Micrographs of the fracture surfaces at the central region (the arrow in the inset shows the exact point where the SEM image was taken from) of specimens of the four materials tested at 23 °C.

transition to lower T (under plane-strain, the homopolymer shows T_g to be around 0 °C, and the copolymers between −80 and −20 °C [12–14]). At −40 °C, H0 shows unstable and quasi-brittle fracture, Fig. 2(a), with three distinct regions: a smooth ductile and stable growth region near the notch, a rough unstable region immediately after, and a final region of brittle fracture (although this is not shown in Fig. 2(a)).

4.1.1. Influence of ethylene content on the fracture surface deformation

Figs. 3 and 4 show the fracture surfaces of the central regions of the materials tested at 23 and −40 °C, respectively. For comparison, it is important to take into account that in one case (23 °C, Fig. 3), H0 gave higher toughness, whilst in the other case (−40 °C, Fig. 4), the EPBC had better EWF properties. Also note that, as expected, one main difference between Figs. 3 and 4 is the size of the deformed region (and consequently, the total deformation to fracture). In Fig. 3, the central region of the four materials deformed at 23 °C is shown at a lower magnification. It is shown that whereas H0 shows a very flat and smooth fracture surface, its roughness increases markedly with EC. Also note the thickness reduction, independent of the EC, changes from ~90 µm to about one-third of this value after fracture for all materials tested.

Fig. 4 shows the central region of the four materials fractured at −40 °C. In Fig. 4(a), the rough region of H0 is enlarged, revealing that only very little plastic deformation has occurred, probably associated with multiple crazing. This result has also been observed at high loading rates at ambient temperature [15]. The surface roughness is believed to be caused by simultaneous propagation of multiple crazes originated at different planes. Note that this region is not the main feature in H0 at this T; but the completely brittle surface is, where plastic deformation is almost non-existent. Thus, it can be stated that fracture of H0 at the lowest T involves a combination of energy dissipative deformation mechanisms of multiple crazing and shear-yielding (which occurs during the formation of shear lips at the initial stage of the test). Conversely the copolymers, with ductile and stable fracture at any T, show a completely different fracture surface as shown in Fig. 4(b)–(d). Comparing these figures which correspond to the fracture features of

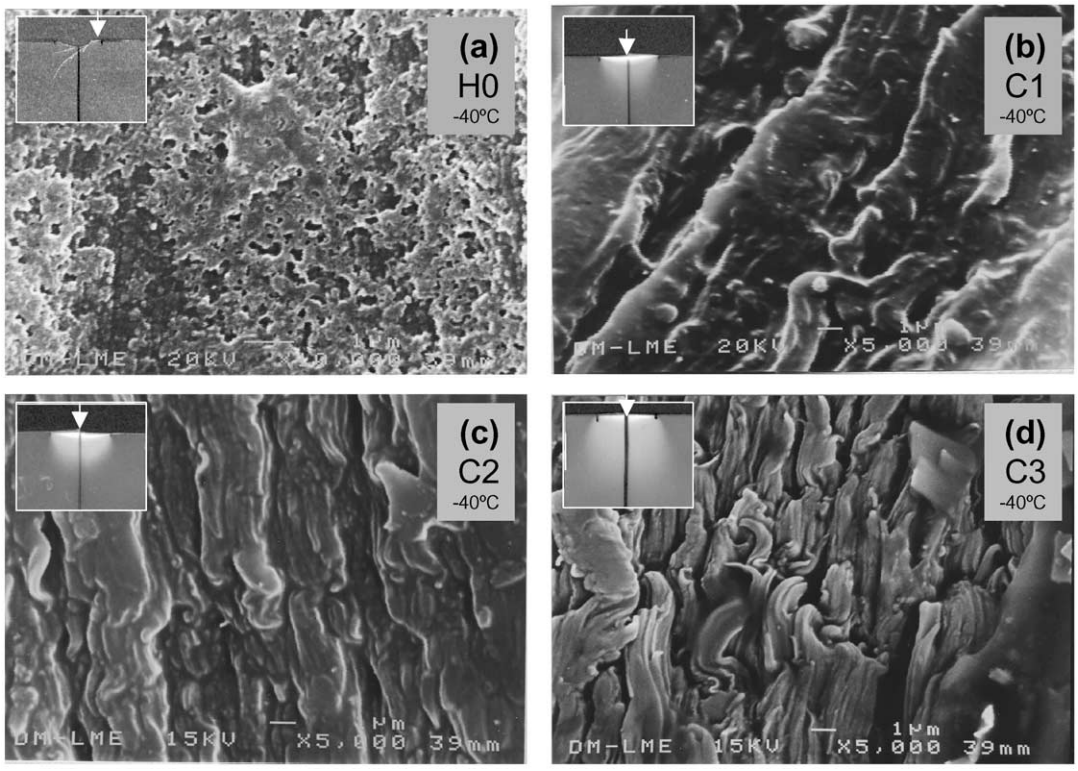

Fig. 4. Micrographs of the fracture surfaces at the central region (the arrow in the inset shows the exact point where the SEM image was taken from) of specimens of the four materials tested at −40 °C.

C1, C2 and C3, it can be seen that for low EC, the surface is very flat, and as EC increases, the plastic deformation also increases. This suggests that the work dissipated at the actual fracture path for the creation of two new surfaces should increase with EC.

4.1.2. Influence of temperature on the fracture surface deformation

To analyse the effect of T, Figs. 5 and 6 show the same material (C2 in both cases) at different T, taken from different fracture surface regions (central and notch, respectively). By observing the fracture surface of different specimens, an important evolution as T varies is noticed. In Fig. 5, SEM micrographs taken from the central region of a C2 specimen fractured at three different T are shown. The differences are clear in that the amount of deformation at the fracture surface is much more pronounced as T rises. An orientation of the deformed structure can also be seen, which coincides with the tearing direction. Fig. 6 shows pictures taken on the same material from the notch region (note that T are not exactly the same as in Fig. 5), and a similar evolution with T can be seen. However, it appears that the deformed region shows more 'cavitation' in the notch region than in the central region. It is noted that the tear propagation is rather slower at the beginning of the test (near the notch) than at the end (central region), thus producing different deformation characteristics of the fracture surface. By comparing these figures with those in Section 4.1.1, it can be concluded that increasing T has a similar influence as increasing EC. However, while at lower T the surfaces show smaller amount of plastic deformation (Figs. 5(c) and 6(c)), at higher T the plastic deformation increases markedly, showing a well-developed fibrillar and cavitated structure, especially at 50 °C (Fig. 6(a)). Comparison of the broken specimens reveals that the thickness reduction depends on T, being larger as T is increased (this can be deduced from the total deformation of the specimens after fracture as given in the insets of figures). However, the effect of T on the homopolymer is different compared to the copolymers as discussed in Section 4.1.1. There is a ductile–brittle transition at $T < -20$ °C, and ductile fracture with low plastic deformation at higher T.

4.2. SEM observation of deformed sections

In our previous work [9], the different zones surrounding the fracture path were analysed carefully. As usual, when applying the EWF theory, two areas can be defined: FPZ and OPZ. For the copolymers, the latter was found to be divided into an intense and a diffuse stress-whitened outer plastic zone (IOPZ and DOPZ, respectively). This phenomenon has already been reported by other authors in thick plates of modified PP [16–18]. Both zones were especially visible in the specimens tested at low T, and were formed during different stages of the fracture process. The creation of both zones during the whole test can be observed in Fig. 7,

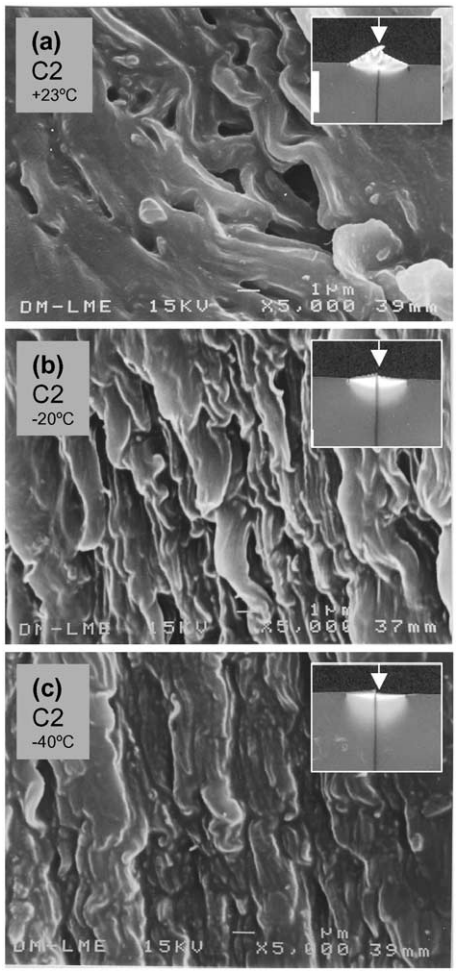

Fig. 5. Micrographs of the fracture surfaces at the central region (the arrow in the inset shows the exact point where the SEM image was taken from) of C2 specimens tested at three different temperatures: (a) 23, (b) −20, and (c) −40 °C.

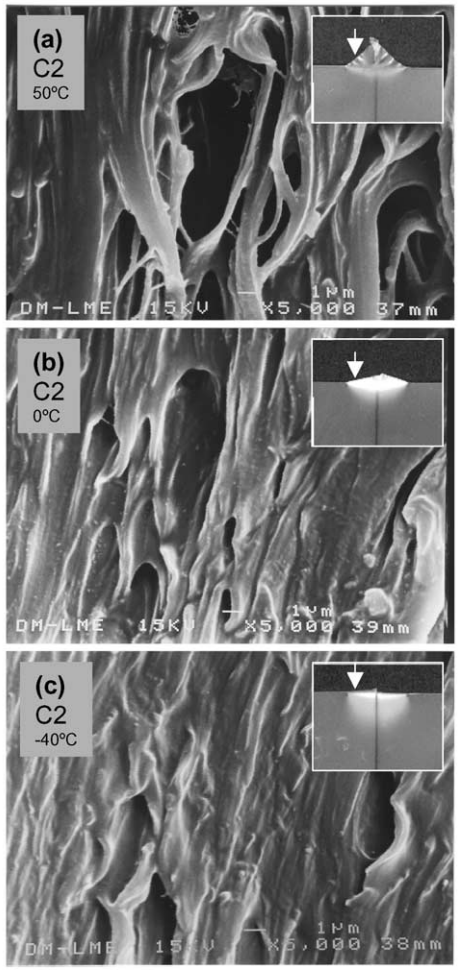

Fig. 6. Micrographs of the fracture surfaces at the notch region (the arrow in the inset shows the exact point where the SEM image was taken from) of C2 specimens tested at three different temperatures: (a) 50, (b) 0, and (c) −40 °C.

where micrographs were taken at different loading stages during the fracture test of a C1 DENT specimen at −40 °C. Note that for better observation of the evolution of the IOPZ and DOPZ sizes, the load was released before taking each picture, which explains why the crack opening is always very small and the crack advance is difficult to be appreciated. Nevertheless, it can be seen that at maximum load (Fig. 7, picture D), the DOPZ is completely formed, without having consumed almost any plastic work (since this occurs at approximately the end of the linear-elastic region). It was observed that the formation of the IOPZ takes place during the whole fracture process and not until the maximum load only. Actually, the IOPZ grows into the previously formed DOPZ, as tearing continues (although it is difficult to see, tearing starts after the maximum load around point E [9,19]). Another remark reported in our previous work [9] was that the size of the DOPZ increased with decreasing T. A similar observation, due to increasing test speed, was found recently in impact testing of impact-modified PP using compact-tension specimens [15]. These authors suggested that under impact conditions (or low T), deformation processes were activated in a significantly larger sample volume. Although it is of interest to understand this phenomenon, it is of secondary importance since the consumed work in the DOPZ is very small.

SEM observations of sections of deformed specimens (schematics in Fig. 1(b)) illustrate the differences between the IOPZ and DOPZ. Fig. 8 shows the interior sections of fractured C1 and C3 specimens at 0 °C obtained from both the IOPZ and the DOPZ. Clearly, in these copolymers, stress-whitening is due to the appearance of a large number of holes ~1 μm diameter in the bulk material. These microvoids appear initially in the DOPZ and are spherical (Fig. 8(b) and (d)). As the deformation increases, the spherical holes grow in the tensile direction, becoming elongated and coalesce with neighbouring holes. This second deformation step probably occurs by shear-yielding. The result is an increase in the intensity of stress-whitening, which macroscopically is the IOPZ (shown in the sequential photographs in Fig. 7). The literature has treated deeply this topic in

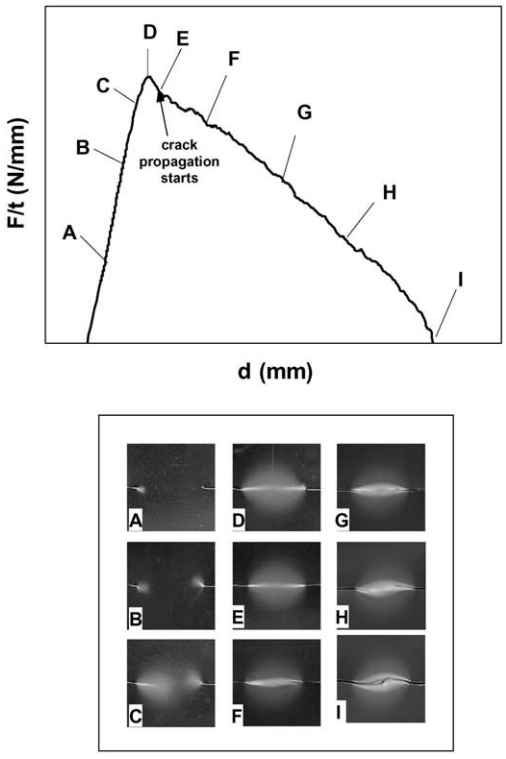

Fig. 7. (a) Load–displacement curve of a C1 DENT specimen tested at −40 °C. (b) Images taken from the ligament area of the tested specimen at the different stages of the fracture test indicated in (a). Note that the specimen was unloaded before taking each picture.

different rubber-toughened systems, identifying cavitation/shear-yielding as major toughening mechanisms in non-crazing materials [16–18]. However, controversy still remains as to which is the more predominant mechanism. On the contrary, H0 does not show any voiding, suggesting that these micro-voids are produced by the second (ethylenic) phase. Thus, unless it is in the brittle *T* range and shows a crazing mechanism, PP homopolymer deforms by shear-yielding without cavitation with no stress-whitening visible.

4.2.1. Influence of temperature on bulk deformation

Fig. 9 shows the influence of temperature on the deformation of core region of the IOPZ at three distinct *T*. The arrows in the insets show that the SEM photos are taken according to Fig. 1(b). Clearly, for the copolymers, at −40 °C, some spherical holes appear (see Fig. 9(a)), which are not deformed even in the IOPZ. At 0 °C (Fig. 9(b)), the initial spherical micro-voids have been deformed along the tensile direction, and their density increases. At 50 °C, no holes are seen; nor is there any stress-whitening. These findings can be explained as follows. So long as both phases present are in a *T* range above their glass transition temperatures (T_g), homogeneous deformation is possible, and no separation between them occurs (Fig. 9(c)). However, at −40 °C, the propylene phase deformation is restricted, as *T* is below its glass transition ($T_g^P \sim 0$–20 °C), and the ethylene phase is above its T_g. Thus, the difference in the deformation capacity produces a

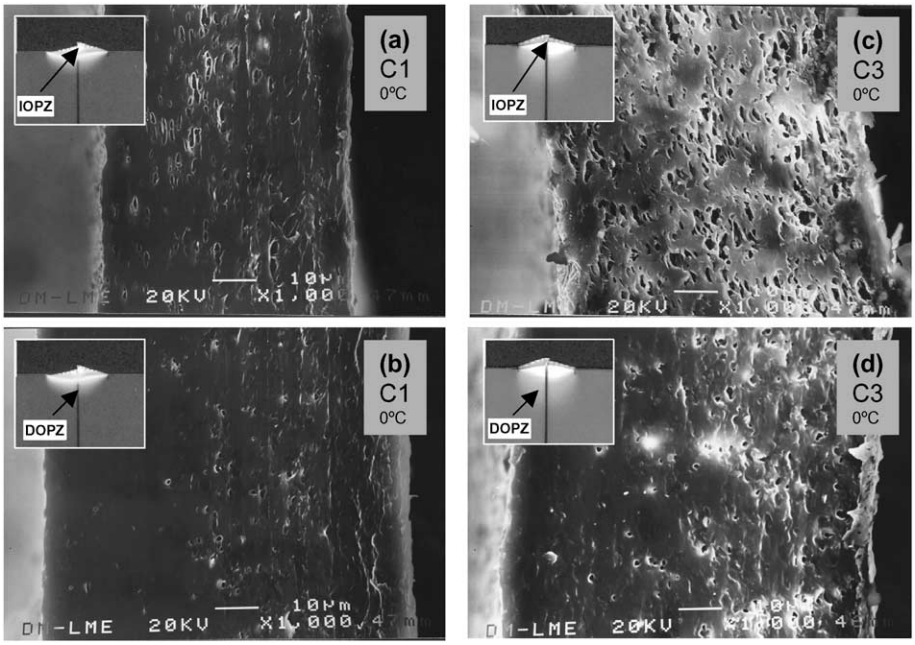

Fig. 8. Micrographs of the core regions (the arrow in the inset shows the exact point where the SEM image was taken from) of specimens of C1 and C3 tested at 0 °C. (a) and (c) correspond to the IOPZ, and (b) and (d) to the DOPZ.

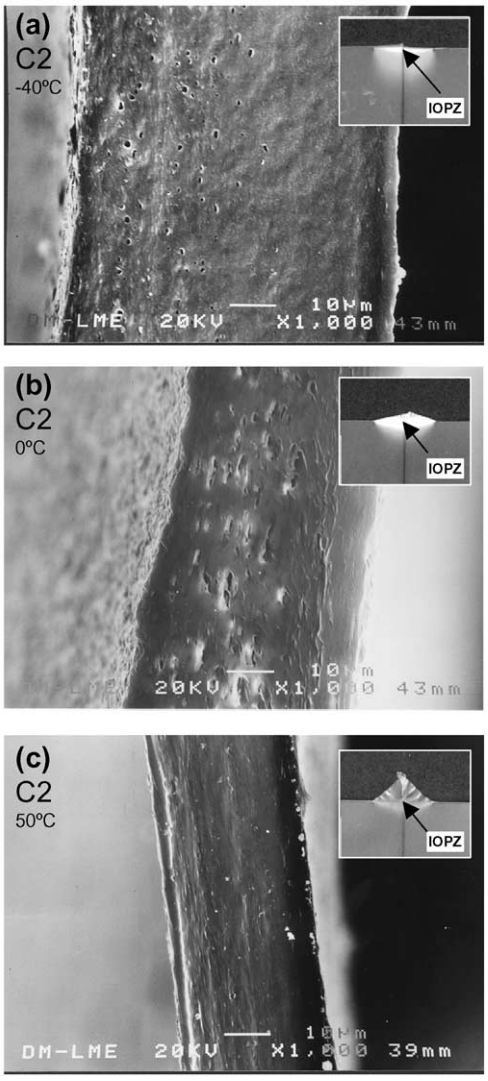

Fig. 9. Micrographs of the core regions in the IOPZ (the arrow in the inset shows the exact point where the SEM image was taken from) of C2 specimens tested at (a) −40, (b) 0, and (c) 50 °C.

Fig. 10. SEM micrographs of the section of a H0 specimen tested at 0 °C, showing the neck region (the arrow in the inset shows the exact point where the image was taken from).

heterogeneous deformation in the core region (Fig. 9(a)), accompanied by cavitation with spherical voids. An intermediate case is found at 0 °C (Fig. 9(b)), where even though heterogeneous deformation occurs (producing cavitation), the PP *matrix* also displays large deformation, which is represented by the micro-voids becoming elongated with a substantial reduction of the sample thickness from 90 to about 40 μm.

It is also noted from many SEM micrographs, for example Figs. 8(b) and (d) and 9(a) and (b), that the holes are not uniform across the section thickness but are more located on one side of the film. We believe that this is caused by the asymmetrical morphology of the film due to the transformation process. After extrusion, the cooling process took place in the rolls firstly on one side of the film resulting in a different microstructure between the two sides. Whilst we consider that this heterogeneity does not affect significantly the conclusions of our work, further studies are being carried out to ascertain the results.

4.2.2. Influence of ethylene content on bulk deformation

An obvious conclusion regarding the effect of EC is that no stress-whitening is observed in H0. Fig. 10 shows necked down region in a H0 specimen at 0 °C and no cavitation appears in the bulk material, thus indicating that shear-yielding may be the only deformation mechanism when ductile fracture occurs. But the copolymers show clear stress-whitening produced by cavitation, Fig. 8, and the EC determines the density of micro-voids, being higher as EC increases, in both DOPZ and IOPZ.

4.3. Relationships between EWF parameters and SEM observations

In Sections 4.1 and 4.2, fractographic results have been shown and discussed. But it is more important to relate these observations to the EWF parameters, w_e and βw_p, for the same materials as reported in our previous work [9], Fig. 11. In summary, the EWF parameters of the homopolymer were shown to be much more temperature-sensitive than EPBC with lower EWF values at $T < T_g$ and the opposite trend at $T > T_g$. Conversely, the ductile–brittle transition of the homopolymer that occurs below its T_g was suppressed for the EPBC in the temperature range studied.

For the temperature range below T_g^P (glass transition for propylene), it has been shown in Sections 4.2.1 and 4.2.2 that multiple crazing appears in H0 at $T < -20$ °C, producing brittle fracture with a low fracture energy, although it should be kept in mind that the EWF methodology is not applicable at −40 °C. The presence of a small amount of ethylene in the material (synthesised as a copolymer) is responsible for the existence of high-energy deformation mechanisms as cavitation and shear-yielding, since plastic deformation can take place in the ethylene phase which is well above the T_g^E (glass transition for ethylene). These

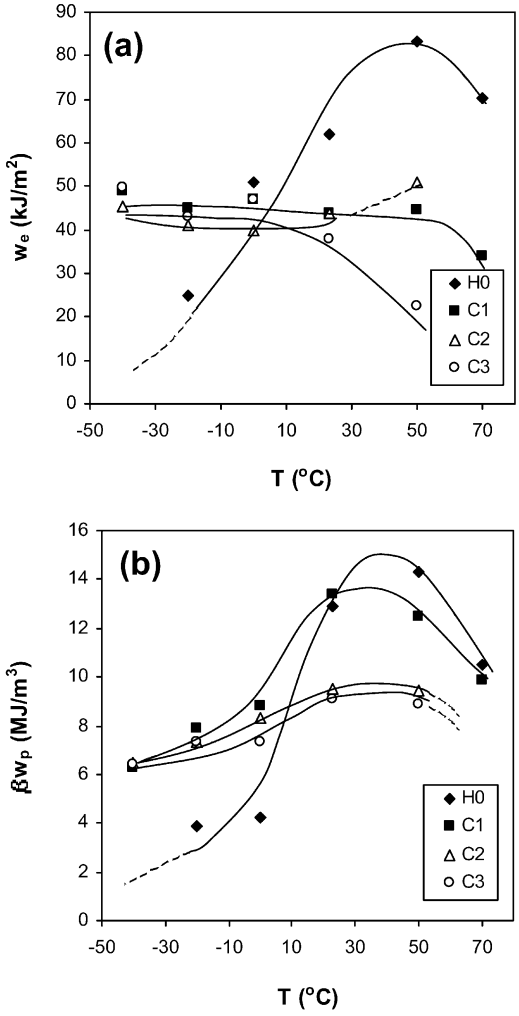

Fig. 11. Evolution of (a) w_e and (b) βw_p with test temperature for the four materials studied.

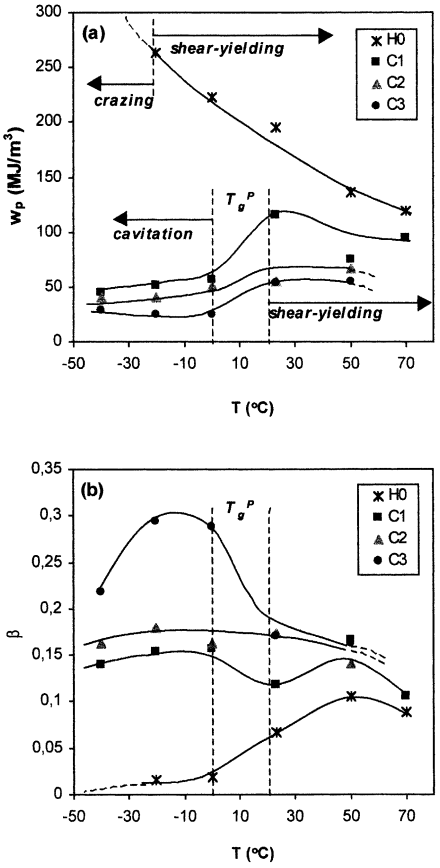

Fig. 12. Evolution of (a) w_p and (b) β with test temperature for the four materials studied. The prevailing deformation micro-mechanisms, and the glass transition range are indicated.

findings are consistent with the fracture parameters calculated (Fig. 11), where low w_e and βw_p values have been obtained for H0 at $T < 0$ °C, in comparison to the EPBC. But no substantial differences in w_e and βw_p exist between these three copolymers, indicating that an increase in the EC, and thus in the cavitation phenomenon, as shown in Section 4.2.1, does not necessarily involve an increase of w_e. Nevertheless, the case of H0 at −20 °C should be particularly considered, since despite only shear-yielding acts as a mechanism (very few crazes were observed and then only in some specimens) the global dissipated energy is very low due to the poor deformation capacity (T is below T_g^P and thus the chain mobility is very low), giving very low w_e and βw_p values.

At $T > 0$ °C, w_e is clearly higher for H0 compared to the copolymers, but the difference is more gradual for the plastic work (βw_p). H0 and C1 show similar plastic work, but C2 and C3 give lower values. In this T range, much of the work is dissipated by shear-yielding since cavitation does not occur at $T >$ ambient temperature (see Fig. 9). At the same T, the shear-yielding mechanism is less prominent in an ethylene-rich copolymer.

It is noted the hypothesis that the term w_e involves more work dissipation than that needed to create just a pair of new surfaces [6,19–21] is supported by the observation that, at high T, H0 gives higher w_e for a flat fracture surface (which involves in theory very low fracture work) compared to the copolymers (see Figs. 3 and 10). Ligament yielding and localised necking always form parts of the total specific EWF, w_e. As shown in Ref. [21], these two terms involve complicated expressions with work-hardening exponent, process zone width, yield stress and crack-tip opening displacements, all of these depend on T, and it is not easy to see the trend of w_e varying with T simply by observing the deformations of the fracture surfaces.

Another important feature is the evolution of the plastic work with T. It can be seen in Fig. 11(b) that, for all materials, βw_p increases with T going through a peak around 40 °C. The evolution of βw_p is related to the variations in the size of the region in which this energy is consumed (primarily IOPZ, as demonstrated previously), represented by β, and the specific non-EWF, w_p (with units of energy per volume unit). In Ref. [9], we determined the dependence

of w_p with T (Fig. 12(a)). It was shown that the homopolymer displayed a decrease in w_p with T in the range studied. But for the copolymers, there were two characteristic regimes divided around T_g^P. Generally, w_p decrease as EC is increased. Above T_g^P, the trend follows H0. Below T_g^P, w_p is less sensitive to but decrease slightly with T. At $T < T_g^P$, cavitation occurs (with shear-yielding), while at $T > T_g^P$, the prevailing mechanism is shear-yielding (without cavitation). Furthermore, one can observe that if cavitation does not occur (as in the homopolymer), no w_p transition appears. However, if at low T, w_p is lower for the EPBC compared to H0, how can the global plastic dissipation energy (βw_p) be superior? The answer lies in the dependence of the plastic zone size (represented by β) with T (Fig. 12(b)). Note that, especially at low T, β is extremely dependent on the EC, imparting much higher βw_p to EPBC than H0. The difference is much less with shear-yielding only.

5. Conclusions

This work shows that fractographic information about energy dissipation mechanisms can successfully explain the variation in EWF parameters for ductile polymeric films, PP and EPBC.

The brittle behaviour of the homopolymer at $T < -20$ °C, with a very low fracture energy, is attributed to the low chain mobility that inhibits shear-yielding and promotes multiple crazing as a dominant mechanism. The stress-whitening effect, only visible for the EPBC at $T \leq$ ambient temperature, has been explained in terms of cavitation. This mechanism only appears in a multi-phase polymer when the deformation is not homogeneous for both phases because one phase is above and the other is below its own glass transition temperature. The cavitation phenomenon is enhanced as the EC is higher, though this does not imply an increase in the fracture parameters.

The main plastic zone in terms of work dissipation is the IOPZ (the DOPZ creation only involves a small amount of work), and is related to the deformation and coalescence of the micro-voids initially created in the DOPZ by cavitation, and matrix deformation by shear-yielding. In the FPZ, the controlling factors for the toughness (w_e) are the mechanisms related to ligament yielding and necking more than to the simple creation of two new surfaces.

The evolution of w_p can be explained in terms of the prevailing deformation mechanisms. For H0, w_p increase with decreasing T until shear-yielding is replaced by crazing. For EPBC, cavitation occurs at $T < 20$ °C and produces a drop in w_p. Above 20 °C, w_p vary in a similar way to H0 because the deformation mechanism is the same (shear-yielding). It is concluded that the global plastic term, βw_p, depends very much on the size of the IOPZ at the low T range.

Acknowledgements

D. Ferrer-Balas is grateful to the CICYT for a doctoral grant, especially for the funds to carry out a research project at the Centre for Advanced Materials Technology (CAMT) at the University of Sydney. The authors wish to acknowledge the Targor Group (Spanish Division) for supplying the materials for testing. Y.-W. Mai also wishes to thank the Australian Research Council for partially supporting the ductile fracture work in Sydney. The authors wish to thank M. Marçal (UPC, Spain) for the SEM analysis, and J. Aurekoetxea (Mondragon Eskola Politeknikoa, Spain) for other experimental details.

References

[1] Mai Y-W, Cotterell B. Int J Fract 1986;32:105.
[2] Wu J, Mai Y-W, Cotterell B. J Mater Sci 1993;28:3373.
[3] Wu J, Mai Y-W. Polym Engng Sci 1996;36:2275.
[4] Chan YWF, Williams JG. Polymer 1994;35:1666.
[5] Hashemi S. Polym Engng Sci 2000;40:132.
[6] Karger-Kocsis J, Czigány T, Moskala EJ. Polymer 1998;39:3939.
[7] Karger-Kocsis J. Macromol Symp 1999;143:185.
[8] Maspoch ML, Ferrer D, Gordillo A, Santana OO, Martinez AB. J Appl Polym Sci 1999;73:177.
[9] Ferrer-Balas D, Maspoch ML, Martinez AB, Ching E, Li RKY, Mai Y-W. Polymer 2000;42:2665.
[10] Cotterell B, Reddel JK. Int J Fract 1977;13:267.
[11] Ferrer-Balas D, Maspoch ML, Martinez AB, Santana OO. Polymer 2000;42:1697.
[12] Karger Kocsis J. Polypropylene. Structure, blends and composites. 1st ed. London: Chapman and Hall, 1995.
[13] Hayashi K, Morioka T, Shigeyuki T. J Appl Polym Sci 1993;48:411.
[14] Fernando PL, Williams JG. Polym Engng Sci 1980;20:215.
[15] Gensler R, Plummer CJG, Grein C, Kausch HH. Polymer 2000;41:3809.
[16] Yee AF. Polym Engng Sci 1977;17:213.
[17] Huang Y, Kinloch AJ. J Mater Sci 1992;27:2753.
[18] Van der Wal A, Gaymans RJ. Polymer 1999;40:6067.
[19] Ferrer-Balas D, Maspoch ML, Martinez AB, Santana OO. Polym Bull 1999;42:101.
[20] Maspoch ML, Hénault V, Ferrer-Balas D, Velasco JI, Santana OO. Polym Test 2000;19:559.
[21] Mai Y-W. Int J Mech Sci 1983;35:995.